

1 Title:

2 **The spatial organisation and microbial community structure of an**
3 **epilithic biofilm**

4

5 Nick A. Cutler^{a*}, Dominique L. Chaput^b, Anna E. Oliver^c, Heather A. Viles^d

6

7 ^a Geography Department, University of Cambridge, Downing Place, Cambridge, CB2 3EN,
8 UK

9 ^b Department of Mineral Sciences, Smithsonian Institution, National Museum of Natural
10 History, 10th & Constitution NW, Washington, DC 20560-119, USA

11 ^c Centre for Ecology and Hydrology, Maclean Building, Benson Lane, Crowmarsh Gifford,
12 Wallingford, OX10 8BB, UK

13 ^d School of Geography and the Environment, Oxford University Centre for the Environment,
14 South Parks Road, Oxford, OX1 3QY, UK

15

16 * corresponding author

17

18 Address: Churchill College, Cambridge, CB3 0DS, UK

19 E-mail: nac37@cam.ac.uk

20 Telephone: +44 1223 336202

21 Fax: +44 1223 336180

22

23 **Abstract**

24

25 Microbial biofilms are common on lithic surfaces, including stone buildings. However, the
26 ecology of these communities is poorly understood. Few studies have focussed on the
27 spatial characteristics of lithobiontic biofilms, despite the fact that spatial structure has been
28 demonstrated to influence ecosystem function (and hence biodegradation) and community
29 diversity. Furthermore, relatively few studies have utilised molecular techniques to
30 characterise these communities, even though molecular methods have revealed unexpected
31 microbial diversity in other habitats. This study investigated 1) the spatial structure and 2) the
32 taxonomic composition of an epilithic biofilm using molecular techniques, namely amplicon
33 pyrosequencing and terminal restriction fragment length polymorphism (TRFLP). Dispersion
34 indices and Mantel correlograms were used to test for the presence of spatial structure in the
35 biofilm. Diversity metrics and rank-abundance distributions (RADs) were also generated. The
36 study revealed spatial structure on a centimetre-scale in eukaryotic microbes (fungi and
37 algae), but not the bacteria. Fungal and bacterial communities were highly diverse; algal
38 communities much less so. The RADs were characterised by a distinctive 'hollow' (concave
39 up) profile and long tails of rare taxa. These findings have implications for understanding the
40 ecology of epilithic biofilms and the spatial heterogeneity of stone biodeterioration.

41

42 Keywords: amplicon pyrosequencing; TRFLP; lithobiontic microbes; green algae; bacteria;
43 fungi; mantel correlograms; rank-abundance distributions

44

45 1 Introduction

46

47 Microbial biofilms are a common feature on both natural rock outcrops and stone buildings.
48 Particular attention has been focused on the biofilms that form on stone buildings, as these
49 communities can have a detrimental impact on both the appearance and physical structure of
50 the stone (Warscheid & Braams, 2000, McNamara & Mitchell, 2005, Scheerer, *et al.*, 2009).
51 However, whilst laboratory work has revealed some of the mechanisms by which biofilm-
52 forming microbes contribute to the biodeterioration of stone, very little is known about the
53 ecology of these organisms. In particular, the spatial structure of stone-dwelling (lithobiotic)
54 microbial communities at sub-metre scales (i.e. the size of masonry building components) is
55 poorly understood, as most previous studies have focussed on the micro- or field/landscape
56 scale (Franklin & Mills, 2010). Furthermore, relatively few studies have used molecular
57 (DNA) techniques to characterise the microbial communities of building stone. To address
58 this knowledge gap, we conducted a high-resolution, molecular study of an epilithic biofilm in
59 order to investigate both small- (centimetre) scale spatial structure and microbial community
60 composition.

61

62 Studies of epilithic biofilms have largely neglected the spatial dimension of lithobiotic
63 communities even though a) many biofilms on buildings are patchy on a scale visible to the
64 naked eye and b) distribution of organisms in space (spatial structure) has been
65 demonstrated to have a profound impact on ecosystem function (Franklin, 2005, Nunan, *et*
66 *al.*, 2010) and hence the patterns and processes of biodeterioration. Microbial communities
67 can obviously vary on very small spatial scales. Gleeson *et al.* (2005), for example, found
68 that lithobiotic fungal communities can vary on the scale of individual mineral grains.

69 Studies have investigated spatial variation on the scale of individual buildings (Rindi & Guiry,
70 2003, Rindi, 2007, Cutler, *et al.*, 2013) or on larger (regional) scales (Gaylarde & Gaylarde,
71 2005). However, there is almost no published work that looks at the intermediate scale of
72 centimetres - metres, i.e. at a level that is of interest to building conservators (Franklin &
73 Mills, 2010). Understanding the factors that structure microbial communities at this scale may
74 shed light on the fundamental ecological processes that affect subaerial, lithobiotic biofilms
75 and their influence on the deterioration of stone.

76

77 Previous studies have described the composition of lithobiotic microbial communities (see,
78 e.g., Gleeson, *et al.*, 2005, Gorbushina, 2007, Gleeson, *et al.*, 2010). Most of this work has
79 focussed on individual taxonomic groups (e.g. Cyanobacteria or fungi) and has been based
80 on techniques such as microscopy and *in vitro* culturing of environmental samples. However,
81 these techniques can only capture a tiny proportion of environmental microbial diversity. For

82 example, it is thought that only 1-10% of environmental microbes can be successfully
83 cultured (Pace, 1997). Modern molecular techniques have been used in a variety of habitats
84 including soil (Acosta-Martinez, *et al.*, 2008, Jones, *et al.*, 2009, Tedersoo, *et al.*, 2010) and
85 marine habitats (Pommier, *et al.*, 2010, Gaidos, *et al.*, 2011), but, with a few exceptions, they
86 have not been systematically applied to building stone (Cutler & Viles, 2010). Typically,
87 molecular techniques reveal levels of microbial diversity much higher than those based on
88 cultured environmental samples.

89
90 Our study was broad in that it encompassed the three main groups of microorganism
91 (hereafter, microorganism types) living on building stone i.e. algae, fungi and bacteria. We
92 applied two, widely used, molecular techniques (amplicon pyrosequencing and terminal
93 restriction fragment length polymorphism (TRFLP)) to describe community structure,
94 concentrating on the two-dimensional arrangement of microbes in a thin biofilm (i.e.
95 predominantly epilithic microbes). In terms of spatial structure, we anticipated that samples
96 close to each other would be more similar than widely-spaced samples in terms of
97 community composition, due to centimetre scale patchiness in the biofilm. We also
98 anticipated low taxonomic diversity, but high taxonomic richness, particularly in fungal and
99 bacterial communities.

100

101

102 **2 Materials and Methods**

103 We used molecular methods to describe the spatial structure and composition of a biofilm on
104 a sandstone slab. Broadly, sample-specific TRFLP was used to ascertain the spatial
105 structure of each microbial group and amplicon pyrosequencing was used to establish
106 microbial community composition.

107

108 **2.1 Sampling**

109 In order to assess potential variation in microbial communities at a centimetre-scale, we
110 sampled a smooth, fine-grained sandstone slab at a high level of spatial resolution. The slab,
111 which had been kept in an exposed location in a stonemason's yard in Oxford, UK, had
112 obvious biological growth on its surfaces but was homogeneous in terms of surface texture
113 and composition. Whilst sampling was carried out during the development of a non-
114 destructive sampling technique for epilithic biofilms described in Cutler *et al.* (2012) the
115 following research is based on new analyses of these samples. We focussed on the epilithic
116 microbial community because surface-dwelling microorganisms are easiest to sample and
117 are likely to have the greatest impact on the appearance of the stone. The sampling regime
118 is described in detail in Cutler *et al.* (2012). Briefly, the surface of the slab was divided into a

119 6 x 4 grid of sample locations (24 samples in total), each measuring 30 x 30 mm and
120 separated from neighbouring sample locations by a buffer zone of 25 mm. A section of sterile
121 adhesive tape was applied to the surface of the stone to collect microbial cells from the
122 biofilm. The biological material on the tape was then analyzed using molecular techniques.
123

124 2.2 Amplicon pyrosequencing and TRFLP

125 A modified CTAB extraction method was used to extract DNA from the tape samples: refer to
126 Cutler et al. (2012) for a detailed protocol. Briefly, subsamples (20 µl) were taken from the
127 DNA extracted from each of the 24 tape samples. These subsamples were pooled and
128 cleaned with a Powerclean kit (MoBio Laboratories Inc, Carlsbad, CA) in accordance with the
129 manufacturer's instructions. The pooled sample was then standardised to a DNA
130 concentration of 20 ng/µl and analysed via tag-encoded FLX amplicon pyrosequencing,
131 utilising a Roche 454 FLX instrument (454 Life Sciences, Branford, CT). The primer set
132 euk516F (5'-GGAGGGCAAGTCTGGT-3'), euk1055R (5'-ARCGGCCATGCACCACC-3') was
133 used for eukaryotes (primarily to characterise algae); the primers ITS1F (5'-
134 CTTGGTCATTTAGAGGAAGTAA-3') and ITS4 (5'-TCCTCCGCTTATTGATATGC-3') were
135 used for fungi and the primers 104F (5'-GGACGGGTGAGTAACACGTG-3'), 530R (5'-
136 GTATTACCGCGGCTGCTG-3') for bacteria. The pyrosequencing was performed at the
137 Research and Testing Laboratory (RTL, Lubbock, TX) based upon RTL protocols.
138

139 Mothur 1.32.1 (Schloss, *et al.*, 2009) was used to process raw sequence data generated by
140 the amplicon pyrosequencing, following the pipelines described in Cutler et al. (2014). Briefly,
141 bacterial 16S rRNA, eukaryotic 18S rRNA and fungal ITS flow files were trimmed and
142 denoised with the mothur implementation of PyroNoise (Quince, *et al.*, 2009). Bacterial and
143 eukaryotic rRNA sequences were aligned using the corresponding SILVA reference
144 alignments (Quast, *et al.*, 2013) and only sequences spanning the targeted regions were
145 kept. Data were denoised by clustering together sequences with 1 bp mismatch per 100 bp,
146 and chimeras were removed using the mothur implementation of uchime (Edgar, *et al.*,
147 2011). Bacterial and eukaryotic rRNA sequences were classified against the SILVA
148 reference databases using the Wang method (Wang, *et al.*, 2007), with a cutoff value of 60%
149 for taxonomic assignment. Sequences were also clustered into operational taxonomic units
150 (OTUs) at the 97% similarity level, which corresponds approximately to the species level. We
151 screened the eukaryotic data and removed OTUs identified as Fungi, Embrophyta and
152 Metazoa, as well as all unclassified Viridiplantae and Charophyta (i.e. only OTUs that could
153 be confidently, if broadly, classified as algae remained).
154

155 For fungal ITS sequences, following denoising, the ITS1 region was extracted using the ITS
156 Extractor tool on the PlutoF Workbench (Abarenkov, *et al.*, 2010, Nilsson, *et al.*, 2010) and
157 sequences shorter than 100 bp were discarded. Chimeras were removed using the mothur
158 implementations of uchime. OTU clustering was carried out from a distance matrix
159 constructed in mothur using pairwise distance values. Sequences were classified against the
160 UNITE+INSDC fungal ITS database (Abarenkov, *et al.*, 2010), modified as previously
161 described (Cutler, *et al.*, 2014), with a cutoff value of 50% for taxonomic assignment.

162

163 All sequence data were uploaded with MIMARKS-compliant metadata to the NCBI Sequence
164 Read Archive under Bioproject number PRJNA260418.

165

166 Alongside amplicon pyrosequencing, we also conducted a fresh analysis of TRFLP data
167 associated with the same samples: refer to Cutler *et al.* (2012) for a full description of the
168 original TRFLP protocols. In principle, amplicon pyrosequencing, or a similar, direct
169 sequencing technique, could be used to analyse spatial structure in microbial communities.
170 However, the large number of samples required for a fine-grained, statistically significant
171 study meant that these techniques were considered too expensive when the analysis was
172 initially performed.

173

174 2.3 Data Analysis

175 Because the TRFLP data were sample-specific, they could be used to investigate spatial
176 variation on a scale of a few centimetres. Patchiness in the abundance of dominant taxa in
177 each microorganism type was assessed by calculating dispersion indices. Morisita's Index,
178 I_M , is a simple, global statistic that quantifies spatial patchiness. If the abundance of an OTU
179 varies randomly in space, the observations follow a Poisson distribution; in this case I_M
180 approximates unity. If abundance has a clumped (under-dispersed) pattern, $I_M > 1$.

181 Conversely, in a regular (over-dispersed) arrangement, $I_M < 1$. The deviation from random
182 expectation ($I_M = 1$) can be tested using critical values of the Chi-squared distribution with n -
183 1 degrees of freedom. In this way, Morisita's index may be used to detect the presence of
184 spatial structure.

185

186 The spatial structure of the epilithic community was also investigated with correlograms.
187 Correlograms indicate the degree of spatial correlation between samples at different
188 separation distances (Legendre & Legendre, 1998). In this case, the degree of correlation
189 between samples at different locations was summarised by the Mantel statistic (Mantel,
190 1967). The Mantel statistic indicates the degree of correlation between two matrices,
191 specifically, the correlation between a matrix of ecological dissimilarity and a matrix of

192 geographical distances (i.e. the physical separation between sample locations) derived from
193 the same community. The significance of the Mantel statistic was estimated by means of
194 permutation tests involving 999 randomisations of the ecological distance matrix. The Mantel
195 correlograms were implemented using the *mantel.correlog* function in the *vegan* package
196 (Oksanen, *et al.*, 2011).

197

198 Percent similarity (*PS*) was calculated from presence-absence data extracted from the
199 TRFLP analysis and used to compare community composition across all the sampling
200 locations for each microorganism type separately. Percent similarity is a metric based on
201 similarities in community composition (Faith, *et al.*, 1987). In principle, *PS* figures provide an
202 indicator of spatial heterogeneity in the microbial communities. High mean *PS* between
203 samples implies a spatially homogeneous community (essentially the same taxa are
204 observed in different locations). Conversely, low mean *PS* implies a relatively high degree of
205 spatial variation in community composition, i.e. there are marked differences in community
206 composition from location to location.

207

208 The overall taxonomic diversity for each microorganism type, expressed in terms of the
209 Shannon index, *H*, and Simpson's index, *J*, was calculated from the pyrosequencing analysis
210 (Hill, *et al.*, 2003). Community structure was investigated with rank-abundance plots which
211 illustrated both taxonomic richness and evenness. Rank-abundance distributions (RADs)
212 have been used to infer the mechanisms that underlie community diversity (Tokeshi, 1993,
213 McGill, *et al.*, 2007). Microbial communities have been found to follow several different
214 distributions. Curves describing distributions frequently reported in published literature (i.e.
215 geometric, lognormal and power law models) were fitted to the pyrosequencing data using
216 the *rad.fit* function in the *vegan* package (Oksanen, *et al.*, 2011).

217

218

219 **3 Results**

220

221 **3.1 Spatial structure**

222 Each microorganism type was dominated by just a handful of taxa: for example, the taxa
223 illustrated in Fig. 1 accounted for 41% (algae), 68% (fungi) and 40% (bacteria) of total
224 abundance in their respective categories. The abundance of the dominant OTUs varied
225 across the surface of the slab (Fig. 1). Morisita indices were calculated for each of these
226 OTUs (values given on Fig. 1). In each case, a highly significant degree of under-dispersion
227 (clumping) was observed ($p < 0.001$), with the most marked clumping in the eukaryotic
228 OTUs. At a community level, diversity varied across the surface of the slab in a similar

229 fashion (results not shown). Fungal and bacterial diversity were positively correlated: sites
230 with high fungal diversity also tended to have high bacterial diversity (Spearman rank
231 correlation: $r = 0.4$, $p = 0.05$). Algal diversity was uncorrelated with bacterial and fungal
232 diversity (Spearman rank correlation: algal-fungal $r = 0.3$, $p = 0.14$; algal-bacterial $r = -0.1$, p
233 $= 0.69$). The mean *PS* figure for the algal samples was very high (~90%). Bacterial
234 communities exhibited intermediate levels of *PS* (64%). The figure for fungal communities
235 was lower (50%).

236

237 Fig. 1

238

239 The Mantel correlograms based on the TRFLP analysis indicated significant spatial structure
240 in algal and fungal samples ($p < 0.05$) (Fig. 2). Positive correlation was observed at the
241 smallest spatial scale (< 8 cm) in these samples (Fig. 2a, b). No significant spatial structure
242 was apparent in the bacterial communities (Fig. 2c).

243

244 Fig. 2

245

246 3.2 Community composition

247 A total of 74 algal OTUs, 244 fungal OTUs and 486 bacterial OTUs were identified by
248 amplicon pyrosequencing (Table 1). The proportion of singletons was high in each case
249 (34% of algal reads, 60% of fungal reads and 54% of bacterial reads).

250

251 In total, 2648 reads were classified as algae (Table 2). The sequences were divided between
252 two phyla, the Chlorophyta and the Charophyta. The majority of sequences were associated
253 with the Chlorophyta; sequences from the class Trebouxiophyceae were particularly
254 abundant, accounting for 93.5% of the Chlorophyte reads. Most of these sequences
255 belonged to the Prasiolales. In the Charophyta, the Klebsormidiophyceae were particularly
256 abundant.

257

258 A total of 2626 fungal sequences were analysed. Two fungal phyla, the Ascomycota and
259 Basidiomycota, accounted for 82.1% of these sequences, with each phylum having
260 approximately equal representation (43.9% Ascomycetes, 38.2% Basidiomycetes). Overall,
261 17.9% of fungal reads were unclassified at a phylum level. The sequences from the
262 Ascomycota were overwhelmingly from the subphylum Pezizomycota; the majority of these
263 reads (811 out of a total of 1147) were unclassified below this level. Of the Ascomycete
264 reads classified at a higher level of resolution, sequences associated with the family
265 Capnodiaceae (class Dothideomycetes) were prominent (e.g. the diametiaceous fungi

266 *Cladosporium* sp. and *Batcheloromyces* sp.) In the Basidiomycota, most reads were
267 associated with the Agaricomycotina (915 reads out of a total of 999 Basidiomycetes). The
268 Agaricomycetes accounted for the bulk of these sequences. Lichenised fungi were not
269 detected.

270

271 There were 2401 bacterial reads of which 98.5% were resolved to at least phylum level.
272 Eleven bacterial phyla were represented, however, only three phyla, the Acidobacteria,
273 Actinobacteria and Proteobacteria, accounted for >5% of the total (Table 2). Almost all the
274 Actinobacterial reads were associated with the order Actinomycetales; the sub-orders
275 Frankineae and Pseudonocardinae were notably abundant. Proteobacterial reads were
276 dominated by the Alphaproteobacteria, with the Rhizobiales and Sphingomonadales
277 prominent. However, levels of taxonomic resolution were generally low and most taxa were
278 rare.

279

280 Table 1

281

282 Table 2

283

284 The RADs derived from the pyrosequencing analysis were characterised by high levels of
285 dominance, a distinctive 'hollow' (concave up) profile and long tails of rare species (Fig. 3).
286 Omitting singletons from the rank-abundance plots did not fundamentally change this shape,
287 which closely approximated a zipf (power law) distribution.

288

289 Fig. 3

290

291

292 **4 Discussion**

293

294 **4.1 Spatial variability**

295 The Baas-Becking hypothesis, often summarised as "everything is everywhere - the
296 environment selects" has been a remarkably persistent concept in microbial biogeography
297 (Martiny, *et al.*, 2006). However, the hypothesis does not explicitly address issues of spatial
298 scale and the factors driving the distribution of microorganisms at intermediate scales (from a
299 few centimetres to a few metres) are largely unknown. If the 'everything is everywhere'
300 model applied to our sample slab, then a spatially random distribution of microbes might be
301 expected, given the apparent environmental homogeneity of this surface (in terms of surface

302 texture, meteorological conditions, etc.) However, this was not the case for eukaryotic
303 microbes.

304

305 The mean PS figure for the algae was high, indicating a spatially homogeneous community
306 (at least in terms of species composition): the same taxa frequently co-occurred. Despite
307 this, spatial patchiness over short distances (<8 cm, or approximately equal to the spacing
308 between adjacent sampling locations) was observed. In other words, at this scale each
309 sampling location was positively correlated with adjacent sampling locations, on average. In
310 general terms, spatial pattern in ecological communities can arise due to environmental
311 patchiness (e.g. resource availability or disturbance), contagious ecological processes (e.g.
312 dispersal, reproduction) or a combination of both (Fortin & Dale, 2005) In this case, the
313 observed spatial patchiness may have been related to the contagious spread of an abundant
314 species. In the pyrosequencing analysis, the most abundant OTU was associated with a
315 *Klebsormidium* species, a filamentous alga which could structure the algal community by
316 contagious spread. However, it is more likely that the spatial structure observed represents
317 differences in OTU abundance (i.e. patch intensity), rather than the presence/absence of
318 particular taxa, because community structure was similar across the sampling locations. In
319 other words, what we observed was a compositionally homogeneous community that varied
320 in relative abundance of different species. The contour plot of the dominant algal OTUs (Fig.
321 1), which features pronounced hotspots of abundance, and the I_M values for the same taxa
322 supported this view. Rindi and Guiry (2003) and Cutler et al. (2013) noted that green algal
323 communities can exhibit small-scale spatial heterogeneity. Our results are consistent with
324 these observations. The presence of green algal patches on stone surfaces has been linked
325 to geochemical and geophysical changes in stone (Cutler, *et al.*, 2013), so understanding
326 characteristic scales of variation may assist in understanding patterns of
327 biodeterioration/bioprotection.

328

329 The fungal community had a low mean PS figure. This indicated considerable differences in
330 community composition between sampling locations. The distribution of the most abundant
331 taxa was also highly patchy (Fig. 1). Spatial variation in fungal communities has been
332 described previously (Cutler, *et al.*, 2013) and, as with algae, may be a function of
333 environmental or ecological variation (or both). Like the algae, the fungi exhibited short-range
334 spatial autocorrelation (Fig. 2b). When viewed in the context of low mean PS , this indicates
335 sharp changes in community composition and species abundance across short spatial
336 distances. Spatial pattern in the fungal samples could be due to the short-range development
337 of patchy surface molds, although the low level of taxonomic resolution in many OTUs made
338 it impossible to be definitive. As with algae, fungal activity has been closely linked with stone

339 biodeterioration, so it is likely that the patchy structure of abundant fungal OTUs is closely
340 correlated with patchy discoloration and/or surface degradation.

341

342 The bacterial community had a moderate mean PS value as there was a high level of co-
343 occurrence amongst the dominant OTUs. The I_M values calculated for these OTUs
344 suggested spatial clumping. However, the associated contour plots indicated that the
345 patches were larger and less intense than those observed for the eukaryotes (Fig. 1). The
346 Mantel correlogram, which was based on the whole bacterial community, did not indicate
347 significant spatial structure at the scale of measurement (Fig. 2c). It is possible that spatial
348 structure was present at a scale smaller than the sampling unit. Whereas filamentary
349 microorganisms (e.g. mycelium-forming fungi and certain algal species) may spread widely,
350 the spatial range of assemblages of isolated bacterial cells may be limited. The absence of
351 pattern in the bacterial community contrasted with the algal and fungal communities and
352 suggested homogeneity in species composition and patch intensity. Interestingly, diversity in
353 the heterotrophic fungal and bacterial communities was positively correlated, suggesting
354 diversity 'hotspots' across the surface of the slab. Further study would be required to
355 establish the factors that promote diversity in the heterotrophic community.

356

357 This study only concentrated on the two-dimensional arrangement of microbes in a thin
358 biofilm. Whilst epilithic microbes have an extremely important impact on stone conservation
359 (not least because they can cause surface discolouration), endolithic microbes also play a
360 significant role in stone biodeterioration. Future studies could seek to establish the three-
361 dimensional structure of lithobiontic communities, perhaps by analysing thin, stone sections
362 from different depths at each sampling location.

363

364 4.2 Community composition and structure

365 In taxonomic terms, the microbial community was broadly similar to those previously reported
366 for other stone substrates in temperate climates (e.g. John, 1988, Flores, *et al.*, 1997,
367 Burford, *et al.*, 2003, Rindi & Guiry, 2004). The distinctive hollow shape of the RADs derived
368 from the pyrosequencing data was also familiar from previous studies of microbial
369 communities in different settings (e.g., Gans, *et al.*, 2005, Pommier, *et al.*, 2010, Inceoglu, *et*
370 *al.*, 2011). Therefore, the high-resolution molecular study, whilst it provided additional detail
371 on community composition and diversity, was largely consistent with previous models of
372 microbial community structure.

373

374 4.2.1 Taxonomic composition

375 A review of literature on epilithic algal communities in Western Europe suggests a relatively
376 small pool of widely dispersed, cosmopolitan species (Cutler, *et al.*, 2013). Our results are
377 consistent with this scenario. In common with previous studies, green algae from the
378 Chlorophyta (primarily of the order Trebouxiophyceae) were dominant. Microscopic
379 Charophyta, notably from the order Klebsormidiophyceae, were also abundant.
380 *Klebsormidium* spp. have been routinely reported on stone surfaces in humid habitats (e.g.
381 Ortega-Calvo, *et al.*, 1993, Rindi & Guiry, 2003).

382

383 Several previous studies of lithobiontic fungal communities have indicated dominance by the
384 Ascomycetes (e.g. Gleeson, *et al.*, 2010). This was not the case in our study: the
385 representation of Ascomycetes and Basidiomycetes was only slightly in favour of the former.
386 The relatively high proportion of Basidiomycetes and non-lithobiontic Ascomycetes may
387 indicate a high level of allochthonous material (e.g. spores) across the surface of the slab
388 (this material might be preferentially sampled when adhesive tape is used). Lichenized fungi
389 were unexpectedly absent. Lichens are often found in lithic habitats and poorly
390 developed/degraded (and unidentifiable) lichen thalli were present on the surface of the slab.
391 However, these areas were not directly sampled and it may be that the tape sampling
392 method we used is poorly suited to collecting material from firmly-adhered lichen thalli. In
393 contrast, ubiquitous, diametiaceous hyphomycetes were relatively abundant. Taxa such as
394 *Cladosporium* spp. are frequently observed in lithobiontic habitats (Burford, *et al.*, 2003);
395 *Batcheloromyces* sp. is reported less commonly.

396

397 McNamara and Mitchell (2005) observed that bacterial communities on stone are typically
398 dominated by taxa drawn from five phyla, i.e. the Proteobacteria, Actinobacteria,
399 Bacteroidetes, Acidobacteria and low-GC Firmicutes group. All these phyla were present on
400 the slab, although only Actinobacteria and Proteobacteria were abundant. Bacterial
401 communities on stone are often closely related to soil communities and this was the case in
402 our study. Several authors have commented that Actinobacteria are particularly abundant in
403 temperate biofilms and this observation was consistent with our results (Scheerer, *et al.*,
404 2009). The Proteobacterial taxa found on the slab are cosmopolitan and have been reported
405 in a wide range of habitats, so it is difficult to infer much from their presence.

406

407 4.2.2 Community structure

408 As expected, the bacteria were the most diverse group, followed by the fungi. Algal diversity
409 was relatively low. In both the bacteria and the fungi, the diversity metrics generated from the
410 pyrosequencing study were much higher than the equivalent figures derived from TRFLP
411 data (by a factor of two: Cutler, *et al.*, 2012). This was unsurprising, as DNA fingerprinting

412 techniques such as TRFLP are known to underestimate microbial community richness
413 (Lalande, *et al.*, 2013). Interestingly, Shannon and Simpson diversity for the algae were
414 remarkably similar for both the pyrosquencing and TRFLP data. It appeared that in the case
415 of algae, rare species (undetectable by TRFLP) did not contribute greatly to overall diversity.
416 This suggests that algal community structure may be adequately captured by TRFLP in
417 certain circumstances.

418

419 A number of previous studies have suggested generic models of microbial RADs, including
420 geometric, lognormal and power law models. Jackson *et al.* (2001), for example, reported
421 that a geometric relationship best described early successional bacterial communities in an
422 aquatic biofilm. However, it is likely that simple geometric models only apply where the
423 members of the community are all competing for the same niche (Dunbar, *et al.*, 2002) and
424 this model was a poor fit for our data. Dunbar *et al.* (2002) proposed that the lognormal
425 distribution is better suited to functionally and phylogenetically diverse assemblages and
426 proposed the use of this distribution as a null model for microbial communities. Lognormal
427 RADs can arise from the multiplicative effects of biotic and abiotic factors and this distribution
428 does not necessarily depend on specific biological/ecological mechanisms. Lognormal
429 distributions have been reported in several bacterial communities (Dunbar, *et al.*, 2002,
430 Doroghazi & Buckley, 2008) but did not capture the essential characteristics of the
431 lithobiontic RADs. Our results are most consistent with the power-law distributions that have
432 been observed in a range of microbial communities from different settings (Gans, *et al.*,
433 2005, Pommier, *et al.*, 2010, Inceoglu, *et al.*, 2011).

434

435

436 **5 Conclusions**

437 Lithobiontic communities, especially those dominated by subaerial green algae, have been
438 characterised as low-diversity assemblages (John, 1988). However, our study demonstrated
439 that microbial communities on building stone can be heterogeneous, both in terms of spatial
440 distribution and taxonomic composition. Different components of the microbial community
441 exhibited different spatial patterns. If the results of our study apply more widely, lithobiontic
442 eukaryotes should exhibit spatial structure over intermediate (centimetre) spatial scales, as
443 well as the large- (metre-) scale patchiness often found to be associated with varying aspect
444 and exposure. Spatial structure in lithobiontic bacterial communities, if it exists, is likely to be
445 at a smaller scale than our sampling interval. DNA fingerprinting techniques, despite their
446 inability to detect rare taxa, may be adequate for profiling green algae in these settings.
447 These findings have implications for understanding spatial heterogeneity in the
448 biodeterioration of stone as the observed patchiness of fungal and algal varieties is likely to

449 be correlated with centimetre-scale variation in stone degradation and soiling. Further study
450 is required to elucidate the ecological relationships between the species that comprise these
451 communities and the factors that generate spatial patchiness in eukaryotes, but not
452 prokaryotic microbes.

453

454 **Funding**

455 This work was supported by the Engineering and Physical Sciences Research Council (grant
456 no. EP/G011338/1).

457

458 **Acknowledgements**

459 The authors are grateful for the helpful comments made by two anonymous reviewers. They
460 are also grateful for the assistance of APS Masonry, Oxford, during the preparation of this
461 paper. The Authors confirm there are no conflicts of interest.

462

Accepted manuscript

463 **References**

- 464 Abarenkov K, Nilsson RH, Larsson K-H, *et al.* (2010) The UNITE database for molecular
 465 identification of fungi - recent updates and future perspectives. *New Phytol* 186: 281-285.
 466 Abarenkov K, Tedersoo L, Nilsson RH, *et al.* (2010) PlutoF-a web based workbench for
 467 ecological and taxonomic research, with an online implementation for fungal ITS sequences.
 468 *Evolutionary Bioinformatics* 6: 189-196.
 469 Acosta-Martinez V, Dowd S, Sun Y & Allen V (2008) Tag-encoded pyrosequencing analysis
 470 of bacterial diversity in a single soil type as affected by management and land use. *Soil Biol*
 471 *Biochem* 40: 2762-2770.
 472 Burford EP, Fomina M & Gadd GM (2003) Fungal involvement in bioweathering and
 473 biotransformation of rocks and minerals. *Min Mag* 67: 1127-1155.
 474 Cutler N & Viles H (2010) Eukaryotic microorganisms and stone biodeterioration.
 475 *Geomicrobiol J* 27: 630-646.
 476 Cutler NA, Chaput DL & van der Gast CJ (2014) Long-term changes in soil microbial
 477 communities during primary succession. *Soil Biol Biochem* 69: 359-370.
 478 Cutler NA, Oliver AE, Viles HA & Whiteley AS (2012) Non-destructive sampling of rock-
 479 dwelling microbial communities using sterile adhesive tape. *J Microbiol Methods* 91: 391-
 480 398.
 481 Cutler NA, Viles HA, Ahmad S, McCabe S & Smith BJ (2013) Algal 'greening' and the
 482 conservation of stone heritage structures. *Sci Total Environ* 442: 152-164.
 483 Cutler NA, Oliver AE, Viles HA, Ahmad S & Whiteley AS (2013) The characterisation of
 484 eukaryotic microbial communities on sandstone buildings in Belfast, UK, using TRFLP and
 485 454 pyrosequencing. *Int Biodeter and Biodegr* 82: 124-133.
 486 Doroghazi JR & Buckley DH (2008) Evidence from GC-TRFLP that bacterial communities in
 487 soil are lognormally distributed. *PLOS ONE* 3.
 488 Dunbar J, Barns SM, Ticknor LO & Kuske CR (2002) Empirical and theoretical bacterial
 489 diversity in four Arizona soils. *Appl Environ Microbiol* 68: 3035-3045.
 490 Edgar RC, Haas BJ, Clemente JC, Quince C & Knight R (2011) UCHIME improves sensitivity
 491 and speed of chimera detection. *Bioinformatics* 27: 2194-2200.
 492 Faith DP, Minchin PR & Belbin L (1987) Compositional dissimilarity as a robust measure of
 493 ecological distance. *Plant Ecol* 69: 57-68.
 494 Flores M, Lorenzo J & Gómez-Alarcón G (1997) Algae and bacteria on historic monuments
 495 at Alcalá de Henares, Spain. *Int Biodeter and Biodegr* 40: 241-246.
 496 Fortin M-J & Dale M (2005) *Spatial Analysis - A Guide for Ecologists*. Cambridge University
 497 Press, Cambridge.
 498 Franklin JF (2005) Spatial pattern and ecosystem function: reflections on current knowledge
 499 and future directions. *Ecosystem Function in Heterogeneous Landscapes*, (Lovett GM, Jones
 500 CG, Turner MG & Weathers KC, eds), pp. 427-441. Springer, New York.
 501 Franklin RB & Mills AL (2010) The importance of microbial distribution in space and spatial
 502 scale to microbial ecology. *The Spatial Distribution of Microbes in the Environment*, (Franklin
 503 RB & Mills AL, eds), pp. 1-30. Springer, Dordrecht.
 504 Gaidos E, Rusch A & Ilardo M (2011) Ribosomal tag pyrosequencing of DNA and RNA from
 505 benthic coral reef microbiota: community spatial structure, rare members and nitrogen-
 506 cycling guilds. *Environ Microbiol* 13: 1138-1152.
 507 Gans J, Wolinsky M & Dunbar J (2005) Computational improvements reveal great bacterial
 508 diversity and high metal toxicity in soil. *Science* 309: 1387-1390.
 509 Gaylarde C & Gaylarde PM (2005) A comparative study of the major microbial biomass of
 510 biofilms on exteriors of buildings in Europe and Latin America. *Int Biodeter and Biodegr* 55:
 511 131-139.
 512 Gleeson DB, Clipson N, Melville K, Gadd GM & McDermott FP (2005) Characterization of
 513 fungal community structure on a weathered pegmatitic granite. *Microb Ecol* 50: 360-368.
 514 Gleeson DB, Melville K, McDermott FP, Clipson N & Gadd GM (2010) Molecular
 515 characterization of fungal communities in sandstone. *Geomicrobiol J* 27: 559-571.
 516 Gorbushina AA (2007) Life on the rocks. *Environ Microbiol* 9: 1613-1631.

517 Hill TCJ, Walsh KA, Harris JA & Moffett BF (2003) Using ecological diversity measures with
518 bacterial communities. *FEMS Microbiol Ecol* 43: 1-11.

519 Inceoglu O, Abu Al-Soud W, Salles JF, Semenov AV & van Elsas JD (2011) Comparative
520 analysis of bacterial communities in a potato field as determined by pyrosequencing. *PLOS*
521 *ONE* 6.

522 Jackson CR, Churchill PF & Roden EE (2001) Successional changes in bacterial
523 assemblage structure during epilithic biofilm development. *Ecology* 82: 555-566.

524 John DM (1988) Algal growths on buildings: a general review and methods of treatment.
525 *Biodeterioration Abstracts* 2: 81-102.

526 Jones RT, Robeson MS, Lauber CL, Hamady M, Knight R & Fierer N (2009) A
527 comprehensive survey of soil acidobacterial diversity using pyrosequencing and clone library
528 analyses. *ISME J* 3: 442-453.

529 Lalande J, Villemur R & Deschenes L (2013) A New Framework to Accurately Quantify Soil
530 Bacterial Community Diversity from DGGE. *Microb Ecol* 66: 647-658.

531 Legendre P & Legendre L (1998) *Numerical Ecology*. Elsevier, Oxford.

532 Mantel N (1967) The detection of disease clustering and a generalized regression approach.
533 *Cancer Res* 27: 209-220.

534 Martiny JBH, Bohannan BJM, Brown JH, *et al.* (2006) Microbial biogeography: putting
535 microorganisms on the map. *Nat Rev Microbiol* 4: 102-112.

536 McGill BJ, Etienne RS, Gray JS, *et al.* (2007) Species abundance distributions: moving
537 beyond single prediction theories to integration within an ecological framework. *Ecol Lett* 10:
538 995-1015.

539 McNamara CJ & Mitchell R (2005) Microbial deterioration of historic stone. *Front Ecol*
540 *Environ* 3: 445-451.

541 Nilsson RH, Veldre V, Hartmann M, *et al.* (2010) An open source software package for
542 automated extraction of ITS1 and ITS2 from fungal ITS sequences for use in high-throughput
543 community assays and molecular ecology. *Fungal Ecol* 3: 284-287.

544 Nunan N, Young IM, Crawford JW & Ritz K (2010) Bacterial interactions at the microscale:
545 linking habitat to function in soil. *The Spatial Distribution of Microbes in the Environment*,
546 (Franklin RB & Mills AL, eds), pp. 61-85. Springer, Dordrecht.

547 Oksanen J, Blanchet FG, Kindt R, *et al.* (2011) *vegan: Community Ecology Package*.
548 <http://CRAN.R-project.org/package=vegan>.

549 Ortega-Calvo JJ, Hernadez-Marine M & Saiz-Jimenez C (1993) Experimental strategies for
550 investigating algal deterioration of stone. *Proceedings of 7th International Congress of*
551 *Deterioration and Conservation of Stone, Vol. 1* (Rodrigues JD, Henriques F & Jeremias FT,
552 eds), pp. 541-549. Lisbon, Portugal.

553 Pace NR (1997) A molecular view of microbial diversity and the biosphere. *Science* 276:
554 734-740.

555 Pommier T, Neal PR, Gasol JM, Coll M, Acinas SG & Pedros-Alio C (2010) Spatial patterns
556 of bacterial richness and evenness in the NW Mediterranean Sea explored by
557 pyrosequencing of the 16S rRNA. *Aquat Microb Ecol* 61: 212-224.

558 Quast C, Pruesse E, Yilmaz P, *et al.* (2013) The SILVA ribosomal RNA gene database
559 project: improved data processing and web-based tools. *Nucleic Acids Res* 41: D590-D596.

560 Quince C, Lanzen A, Curtis TP, *et al.* (2009) Accurate determination of microbial diversity
561 from 454 pyrosequencing data. *Nat Methods* 6: 639-U627.

562 Rindi F (2007) Diversity, distribution and ecology of green algae and cyanobacteria in urban
563 habitats. *Algae and Cyanobacteria in Extreme Environments*, (Seckbach J, ed) pp. 619-638.
564 Springer, Dordrecht.

565 Rindi F & Guiry MD (2003) Composition and distribution of subaerial algal assemblages in
566 Galway City, western Ireland. *Cryptogamie Algologie* 24: 245-267.

567 Rindi F & Guiry MD (2004) Composition and spatial variability of terrestrial algal
568 assemblages occurring at the bases of urban walls in Europe. *Phycologia* 43: 225-235.

569 Scheerer S, Ortega-Morales O & Gaylarde C (2009) Microbial deterioration of stone
570 monuments - an updated overview. *Adv Appl Microbiol* 66: 97-139.

571 Schloss PD, Westcott SL, Ryabin T, *et al.* (2009) Introducing mothur: open-source, platform-
572 independent, community-supported software for describing and comparing microbial
573 communities. *Appl Environ Microbiol* 75: 7537-7541.
574 Tedersoo L, Nilsson RH, Abarenkov K, *et al.* (2010) 454 Pyrosequencing and Sanger
575 sequencing of tropical mycorrhizal fungi provide similar results but reveal substantial
576 methodological biases. *New Phytol* 188: 291-301.
577 Tokeshi M (1993) Species abundance patterns and community structure. *Adv Ecol Res* 24:
578 111-186.
579 Wang Q, Garrity GM, Tiedje JM & Cole JR (2007) Naive Bayesian classifier for rapid
580 assignment of rRNA sequences into the new bacterial taxonomy. *Appl Environ Microbiol* 73:
581 5261-5267.
582 Warscheid T & Braams J (2000) Biodeterioration of stone: a review. *Int Biodeter and Biodegr*
583 46: 343-368.
584
585
586

Accepted manuscript

587 **Figure captions**

588

589 Fig. 1: Contour plots indicating the varying abundance (measured in fluorescence units) of
590 dominant OTUs for each microorganism type. I_M = Morisita index; in each case the value is
591 significantly > 1 ($p < 0.001$), indicating a patchy distribution. The white dots indicate sampling
592 locations.

593

594 Fig. 2: Mantel correlograms for each microorganism type; filled circles indicate significant (p
595 < 0.05) correlation in a given distance class.

596

597 Fig. 3: Rank-abundance plots for algal, fungal and bacterial OTUs (each OTU is represented
598 by a point), based on amplicon pyrosequencing. Singletons have been omitted. The taxon
599 ranked 1 is the most abundant in each case. The plots have been fitted with a zipf (power
600 law) model, indicated by a red line.

601

Accepted manuscript

602 **Tables**

603

	No. OTUs	Shannon's diversity, H	Simpson's diversity, J
Algae	74	2.3	0.81
Fungi	244	3.0	0.83
Bacteria	486	4.2	0.89

604

605 Table 1: Diversity metrics derived from amplicon pyrosequencing

606

607

Accepted manuscript

Algae	No. reads	Proportion of reads (%)
Chlorophyta		
Trebouxiophyceae	1454	54.9
Others	101	3.8
Charophyta		
Klebsormidiophyceae	1087	41.0
Others	6	0.2
Totals	2648	100.0
Fungi		
Ascomycota		
Dothideomycetes ^a	314	12.0
Others ^b	840	32.0
Basidiomycota		
Agaricomycetes	965	36.7
Others	39	1.5
Unclassified at phylum level	468	17.8
Totals	2626	100.0
Bacteria		
Acidobacteria		
Acidobacteria	127	5.3
Others	5	0.2
Actinobacteria		
Actinobacteridae	440	18.3
Others	55	2.3
Proteobacteria		
Alphaproteobacteria	1579	65.8
Others	88	3.7
Other bacterial phyla	107	4.5
Totals	2401	100.0

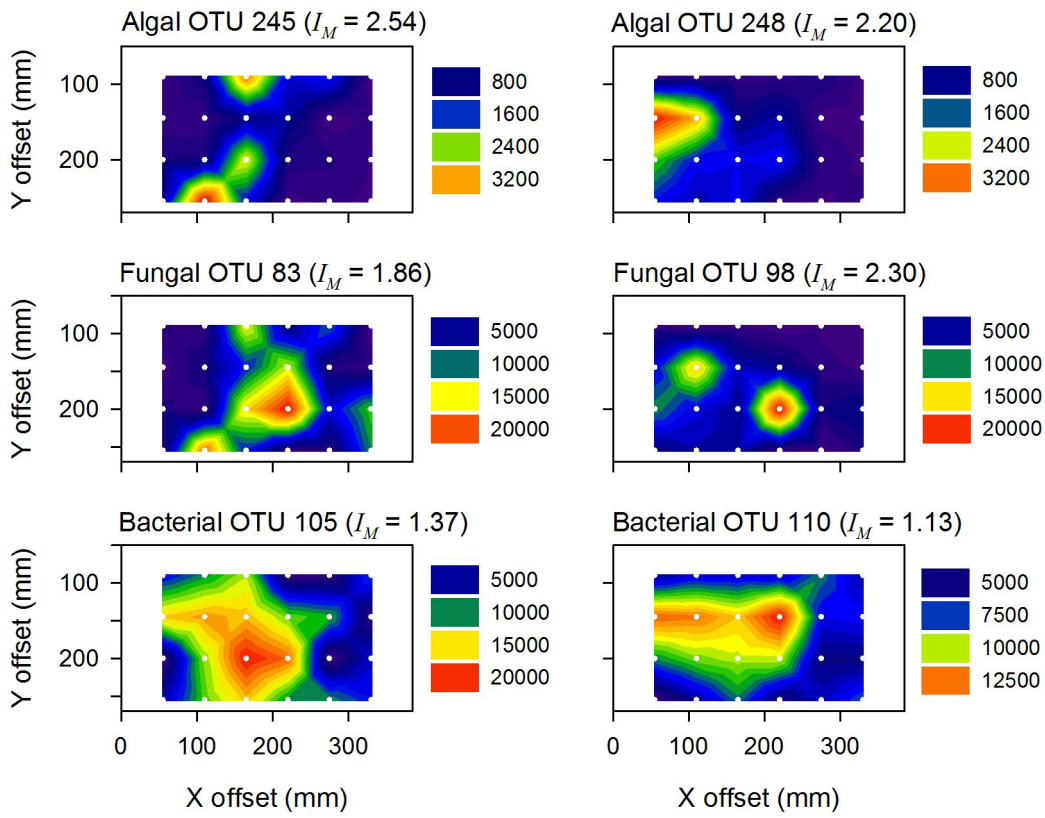
609

610 Table 2: Summary of pyrosequencing results; phyla are indicated with bold text

611

612 **Figures**

613

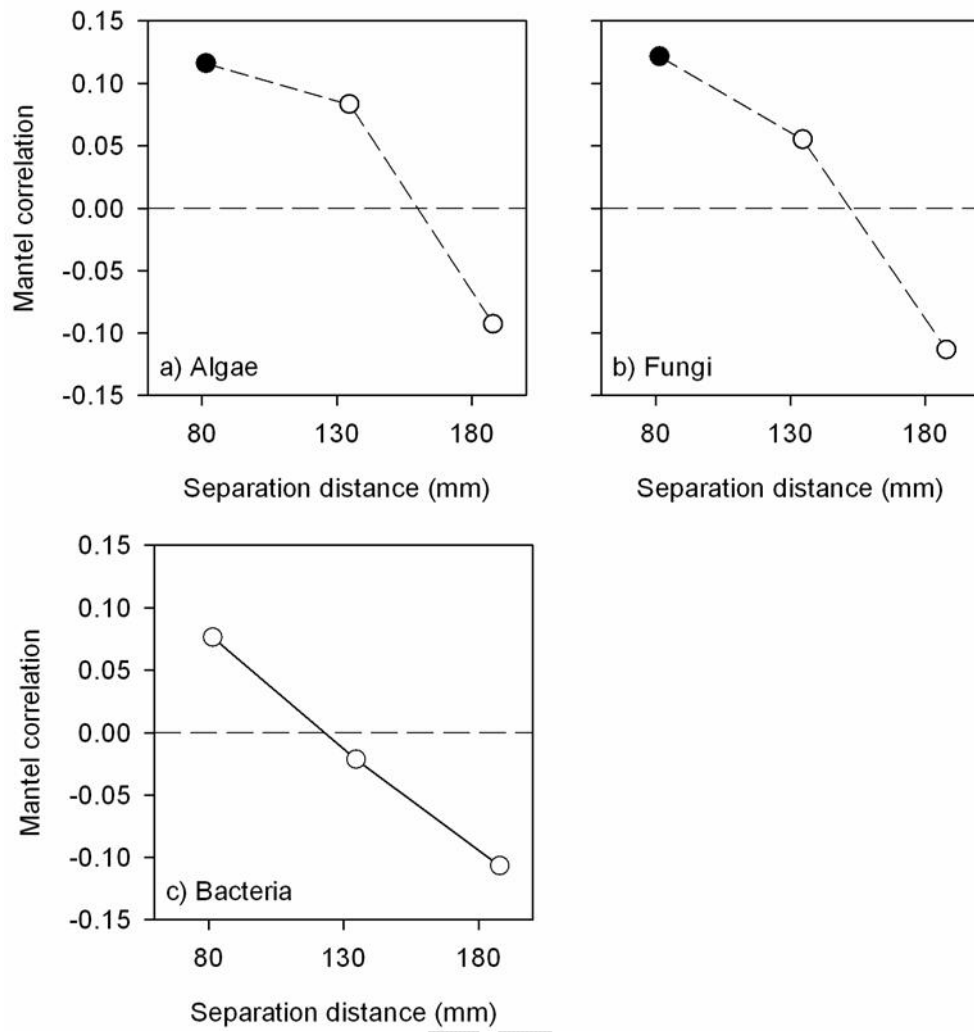


614

615

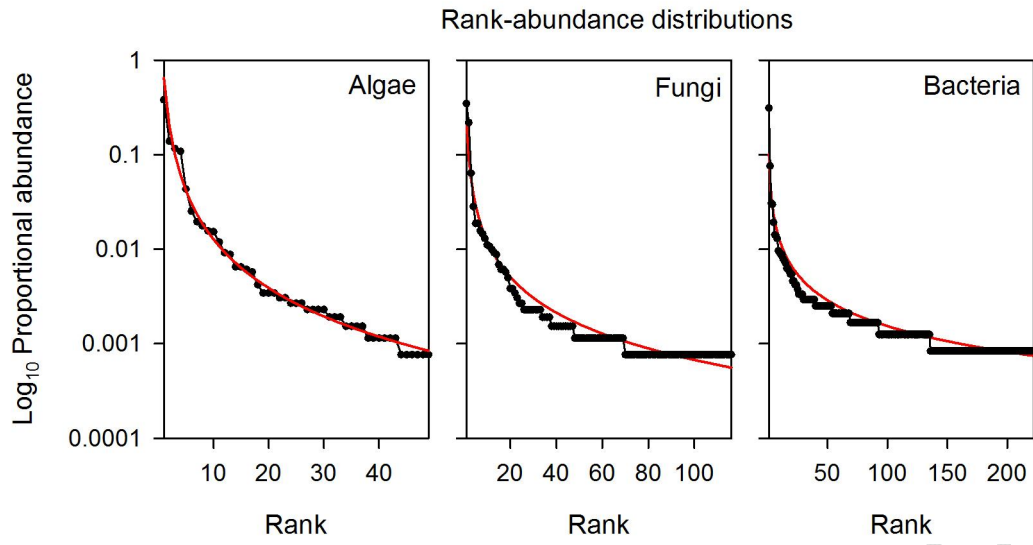
616 Fig. 1

617



618
619
620
621

Fig. 2



622

623

624 Fig. 3

Accepted manuscript